Acta Geotechnica (2021) 16:3761–3778
https://doi.org/10.1007/s11440-021-01399-z

RESEARCH PAPER

A novel multifunctional apparatus for testing unsaturated soils

Kai Liu[1] · Wen-Bo Chen[1] · Jian-Hua Yin[1] · Wei-Qiang Feng[2] · Lalit Borana[3]

Received: 9 June 2021 / Accepted: 11 October 2021 / Published online: 2 November 2021

Abstract

There are limited studies in the development of testing apparatus on unsaturated soils due to the complex structure, tedious calibration process, and large demands on test time and skills. In this study, a novel multifunctional apparatus (MFA) has been designed and manufactured for testing the unsaturated soils. This state-of-the-art testing apparatus is based on modular design and can be configured to conduct a variety of tests such as pressure plate test, oedometer test, direct shear test, and triaxial creep test under suction-controlled conditions. This apparatus has a high-grade stainless-steel chamber which is used to measure the total volume changes of an unsaturated soil specimen in triaxial creep tests. Based on the calibration results, the creep coefficient for MFA is about half of the coefficient for a typical double-cell system. Additionally, the MFA is designed in a manner to enable testing specimens with different dimensions and to control soil suction based on different techniques. Typical calibration results, test procedures, and experimental results obtained from this apparatus are presented and discussed in detail. Finally, the performance of this apparatus is well verified by the experimental results. It is found that the MFA is capable of and reliable for performing above-mentioned tests and accurately investigating engineering behaviour of both saturated and unsaturated geomaterials.

Keywords Direct shear · Multifunctional apparatus · Oedometer · Pressure plate · Triaxial creep · Unsaturated soil

1 Introduction

The water content of soil is usually subjected to seasonal changes when the soil is located above the groundwater table. The water content changes of soil can cause significant variations of soil behaviours such as deformation, shear strength, creep, and stress-strain behaviour, etc. [53]. Whereas unsaturated soil testing is still a big obstacle for researchers and engineers because of the complex and expensive equipment. There are limited studies in the development of testing apparatus on unsaturated soils due to the complex structure, tedious calibration process, and high test demands [37, 38, 52, 53]. The complex structure of apparatus for unsaturated soil testing is designed to fulfil two significant requirements, including independent regulation of pressures of two pore fluids and independent measurement of total volume and water content in soil specimens [5].

In unsaturated soils, the main difficulty to fulfil the first requirement involves regulation and measurement of negative pore-water pressure that cannot be obtained by conventional apparatus without cavitation. Thus, three types of typical techniques have been developed to measure and

✉ Wen-Bo Chen
geocwb@gmail.com

Kai Liu
kevin-kai.liu@connect.polyu.hk

Jian-Hua Yin
cejhyin@polyu.edu.hk

Wei-Qiang Feng
fengwq@sustech.edu.cn

Lalit Borana
lalitborana@iiti.ac.in

[1] Department of Civil and Environmental Engineering, The Hong Kong Polytechnic University, Hong Kong, China

[2] Department of Ocean Sciences and Engineering, The Southern University of Science and Technology, Shenzhen, China

[3] Department of Civil Engineering, Indian Institute of Technology Indore, Indore 453552, Madhya Pradesh, India

control soil suction in the development of testing apparatus on unsaturated soils, including axis translation technique (ATT), osmotic technique (OMT), and vapour equilibrium technique (VET). Total suction of soil can be defined as the summation of matric suction, s, and osmotic suction, π [23]. Typical devices for measuring soil suction are listed in Table 1. Some of the newer methods include chilled-mirror hygrometer and electrical conductivity. The apparatuses and techniques used to measure soil suction vary widely in terms of limitation, time, cost, complexity, and testing range. Table 2 lists typical apparatuses using different techniques to control soil suction, among which the ATT is the most used one. However, the air pressure in ATT cannot represent the field atmospheric condition, and maximum controlled suction is only 1500 kPa [23], which might be low for measuring suction of unsaturated clay, such as bentonite. For the OMT, the field condition can be simulated due to lack of air pressure, and controlled suction can reach up to around 10 MPa [19]. However, the main limitation of OMT lies in the sensitive membranes which is easily attacked by bacteria. Thus, the polyethylene glycol (PEG) solution can infiltrate the specimen and hence the suction cannot be controlled [20]. The main drawback of VET is long period of moisture equalization since vapour transfers based on diffusion [20]. The ATT is adopted in this study for applying relatively low suction on the granular materials, which is adopted for the validation tests.

Other necessities for the tests on unsaturated soils are the independent measurements of total volume and water content changes of a specimen. Total volume change is the main difficulty in unsaturated soil testing since it is related to the changes of pore air and pore water in a specimen. Several measurement techniques have been developed to tackle this problem, including direct air and water volume measurement [1, 35], direct measurement on samples [18, 32], and cell liquid measurement [5, 8, 16, 49, 68]. For the technique of cell liquid measurement, the total volume changes of the specimen are calculated based on volume changes of liquid in the cell. Bishop and Donald [8] proposed a double-cell system, in which mercury was used as the cell liquid in the inner cell. Wheeler [62] developed an improved apparatus with two cells by using a burette to measure the water volume changes of specimen. Yin [68] and Chen et al. [16] developed two new double-cell systems to continuously measure the volume changes of specimens under unsaturated condition and cyclic loading condition, respectively. However, the complexity of these double-cell systems might easily cause possible water leakage, and the Plexiglas of the cell water might absorb water and generate a greater creep effect in the long period in unsaturated soil testing. Agus et al. [2] used a stainless-

Table 1 Overview of the typical devices for measuring soil suction

Device	Suction type	Approximate measurement range (kPa)	Typical references
Filter paper (non-contacted)	Total suction	1000–10,000 or greater	[14, 30]
Psychrometer	Total suction	100–8000	[3, 43]
Relative humidity (RH) sensor	Total suction	7000–70,000	[3]
Chilled-mirror hygrometer	Total suction	1–60,000	[3]
Filter paper (contacted)	Matric suction	0–10,000 or greater	[14, 30]
Null-type axis translation apparatus	Matric suction	0–1500	[39, 48]
Tensiometer	Matric suction	0–1500	[44, 59]
Thermal conductivity sensor	Matric suction	1–1500	[14, 50]
Electrical conductivity sensor	Matric suction	50–1500	[14]
Pore fluid squeezer	Osmotic suction	Entire range	[33]

Table 2 Overview of testing apparatuses using different techniques to control soil suction

Technique of controlling suction	Typical references for oedometer test	Typical references for direct shear test	Typical references for triaxial creep test
Axis translation technique	[5, 52]	[24, 29]	[34]
Osmotic technique	[21, 46]	[12, 25]	Few
Vapour equilibrium technique	[7, 61]	Few	[47]

steel cell to avoid the possible absorption of water. However, the specimen cannot be observed in the test because of the opaque stainless-steel cell. Aversa and Nicotera [5] and Ng et al. [49] proposed aluminium cells and measured water levels by differential pressure transducers. However, the fluid pressure might cause large immediate expansion, and the complexity of the double-cell systems might easily cause water leakage. Thus, it is still necessary to develop a new testing apparatus to tackle the challenges of accurate measurements of volume changes of unsaturated specimens.

Modular design (MD) is a design approach in which product components are produced following a standard and assembled as a system [60]. MD can be used to cope with the complexity of apparatus, massive customization, and expensive cost [6, 31]. So far, there has been little discussion about MD in the development of apparatus on unsaturated soils. Aversa and Nicotera [5] proposed a modular apparatus that can be configured to conduct oedometer and triaxial tests on unsaturated soils. Lauer and Engel [36] developed a triaxial device that can be used to determine shear strength, water retention curve (WRC), and hydraulic conductivity of unsaturated sand. However, these complex apparatuses on unsaturated soils have few functions, and the complexity might cause high cost. The expensive apparatus limits the engineering application of unsaturated soils. MD might help to remove the obstacle of high cost and obtain customization.

In this study, a novel multifunctional apparatus (MFA) on unsaturated soils is developed to conduct pressure plate test, oedometer test, direct shear test, and triaxial creep test for unsaturated soils. This system with stainless-steel cell overcomes the large creep deformation in other typical double-cell systems. Additionally, the MFA is designed in a manner to enable testing specimens with different dimensions and to control soil suction based on different techniques. Compared with a single-function device, an MFA can save a lot of money and space in manufacturing and time for calibration. The detailed set-up, calibration methods, and typical test procedures are introduced. Finally, some typical experimental results on a compacted granular fill are presented to illustrate the performances of this apparatus.

2 Descriptions for the multifunctional apparatus

2.1 General descriptions

A novel MFA for unsaturated soils has been designed, manufactured, and set up in the Soil Mechanics Laboratory of the Hong Kong Polytechnic University (Fig. 1). This apparatus is modular and can be configured to perform different types of tests on unsaturated soils, including pressure plate, oedometer, direct shear, and triaxial creep tests.

2.2 Control of matric suction and net normal stress

A steel hoop with a ceramic disc can be screwed on a custom-built pedestal which can be used in the oedometer-type modified pressure plate module (MPPM) and modified oedometer module (MOM) (Fig. 2a). For the modified direct shear module (MDSM), a steel square plate with ceramic disc can be screwed on a custom-built shear box base (Fig. 2b). In this study, the widely used ATT developed by Hilf [27] was adopted to apply and maintain relatively low matric suction ($u_a - u_w$) on the granular materials. Typically, pore-water pressure, u_w, in unsaturated soils is negative when pore-air pressure, u_a is atmospheric. For the triaxial-type MPPM and modified triaxial creep (MTCM), a steel hoop with ceramic disc can be screwed on a custom-built pedestal (Fig. 2c). The pore-air pressure can be applied and maintained on the coarse porous stone above the specimen through the air pressure pipe on the top of the pressure chamber in MOM and MDSM or air pressure valve on the base in MTCM. For MPPM, both valves on the top (similar to MPPM) and base (similar to MTCM) can be used. The pore-water pressure can be applied and measured by the water drainage system in the water chamber under the high air-entry value disc (HAEVD) which is screwed on the pedestals or shear box base. Exclusive drainage grooves (Fig. 2a to c) have been designed on the pedestals and shear box base to facilitate the circulation of water and the removal of air bubbles under HAEVD. The air-entry values of HAEVDs used in different moduli are 500 kPa. The procedures introduced by Chen [15] were used to prepare the HAEVD before each test.

An axial force can be applied to the specimen by deadweight through the lever and load frame system. The ratio of hanger load to actual applied load on the specimen is 1:24. An inner load cell is linked to the loading piston to measure the axial force directly. A maximum axial force of 26 kN can be applied to the specimens. This force corresponds to stresses of 3.3 MPa on the cylindrical-shaped specimens in MPPM (diameter: 100 mm, height: 100 mm), MOM (diameter: 100 mm, height: 100 mm), and MTCM (diameter: 100 mm, height: 200 mm) or 2.6 MPa on a cuboid-shaped specimen in MDSM (length × width × height: 100.05 × 100.05 mm × 40 mm). A displacement transducer with a range of 50 mm is installed on the loading piston to measure the axial displacement of the specimen.

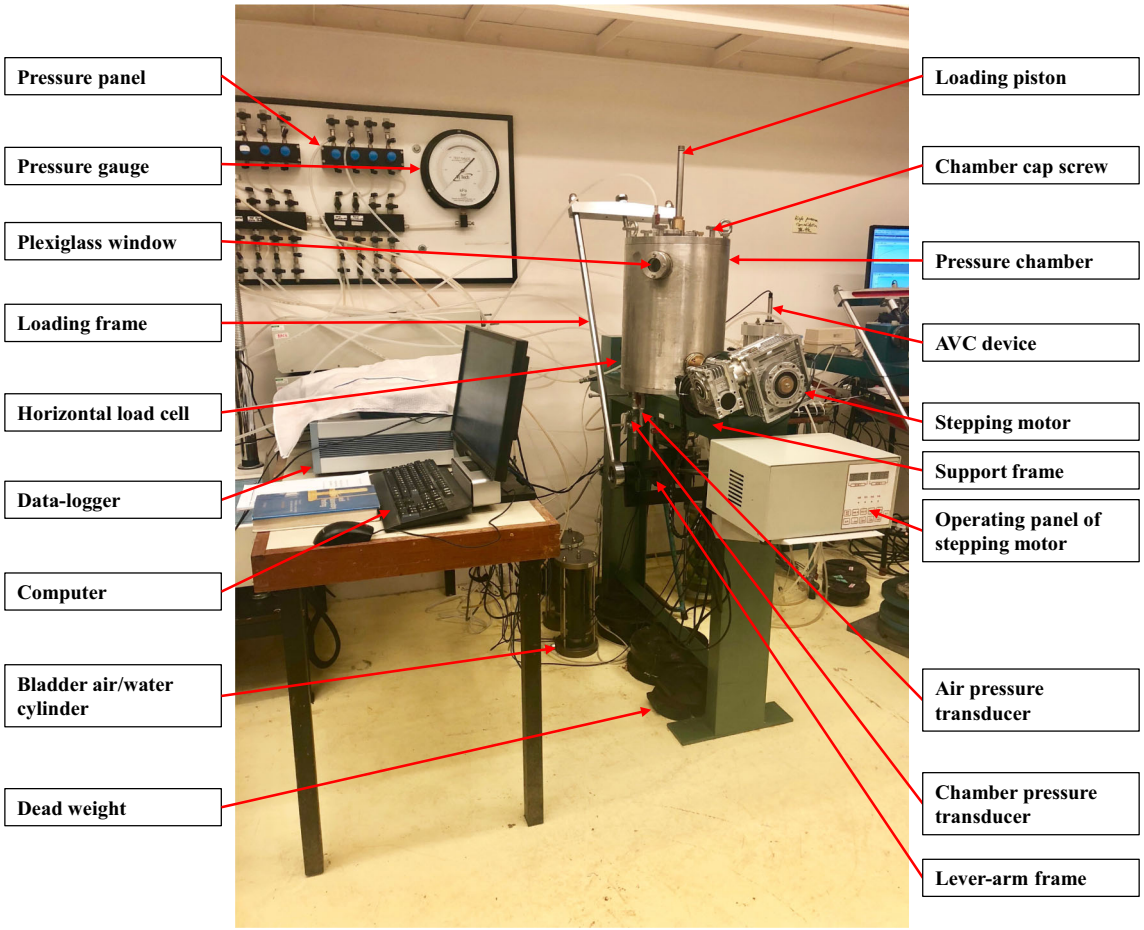

Fig. 1 The multifunctional testing apparatus for unsaturated soils

2.3 Modified oedometer module

The principle of modification for the proposed apparatus is similar to that of the previous relevant developments [5]. As shown in the MOM in Fig. 3, in general, an oedometer apparatus on unsaturated soils is a combination of conventional oedometer and system which can control suction and measure the water content change of specimen. The suction is controlled by the ATT and maintained in the whole loading stage, and load can be applied by the lever-arm frame. The actual load applied to the specimen can be measured by a calibrated inner load cell on the specimen. The deformation of the specimen can be measured by a displacement transducer installed on the loading piston on the specimen. The sample mould used in the specimen compaction can be used as the confining ring in tests. A HAEVD can be screwed on the pedestal at the bottom of the specimen, and a coarse porous stone can be placed on the specimen. The air and water pressures can be applied to the specimen located in the pressure chamber and water chamber under HAEVD, respectively. The drying and wetting of the specimen can be controlled by the changes of matric suction which is associated with water flow in the water chamber. An automatic volume change (AVC) device is connected to the water chamber beneath the HAEVD, and the inflow and outflow of water can be measured. The diffused air under HAEVD can be measured by a diffused air indicator (DAI). The axial force and net stress can be applied to the specimen by the dead weight on the hanger. Before the application of the next loading stage, the stabilization period between each suction or loading change shall be retained until both the water change and vertical displacement keep constant. The two sides of the water chamber are connected to components similar in MPPM. The inner diameter of the pedestal is 100 mm, which is suitable for tests on coarse granular materials. Other pedestals with different diameters can be easily installed on the base of the apparatus for tests on other types of materials.

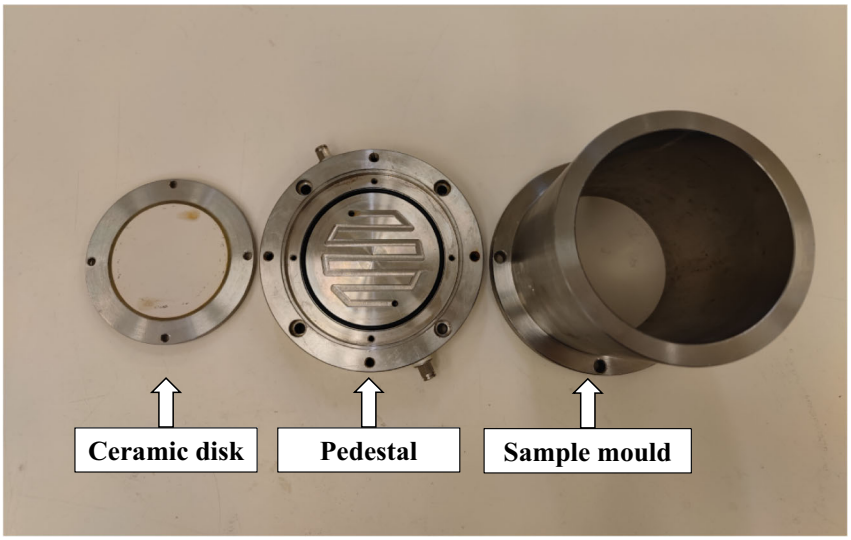
Ceramic disk
Pedestal
Sample mould

(a)

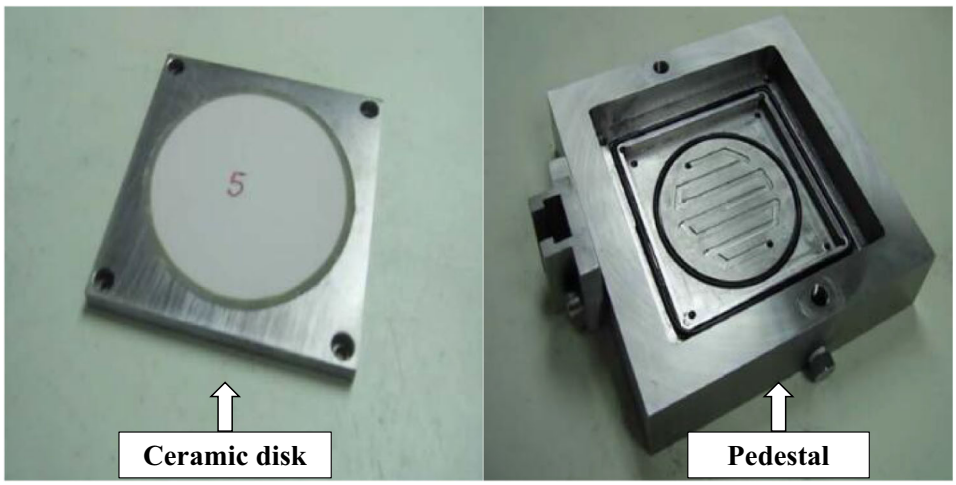
5
Ceramic disk
Pedestal

(b)

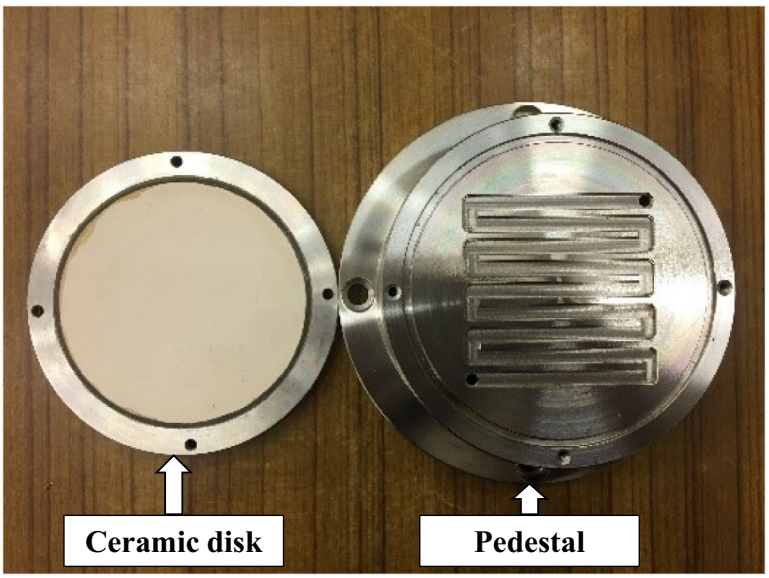
Ceramic disk
Pedestal

(c)

◀**Fig. 2** **a** A custom-built ceramic disc, pedestal, and sample mould used in oedometer-type MPPM and MOM. **b** A custom-built ceramic disc and shear box base used in the MDSM. **c** A custom-built ceramic disc and pedestal used in triaxial-type MPPM and MTCM

Since the horizontal stress of soil specimen is not measured in the current oedometer module, the results shall be interpreted in terms of net vertical stress, σ_v', instead of net mean stress, $\overline{p}$. Nevertheless, the experimental data can still be studied based on the constitutive behaviour of the soils. In any case, compared with other kinds of more sophisticated suction-controlled oedometer apparatus, this apparatus is relatively simple and easy to handle.

2.4 Modified triaxial creep module

The MTCM was designed following a testing apparatus described by Lai et al. [34]. Figure 4 shows the schematic diagram of MTCM. Both the constant shear stress and matric suction can be applied to the soil specimen in the MTCM. The constant shear stress can be applied using dead weights applied to the hanger of the lever-arm frame. To obtain accurate shear stresses, vertical loads applied to a specimen are monitored by an inner load cell in the pressure chamber, which is carefully calibrated before the tests. As stated in "Introduction", based on the technique of cell liquid measurement, the total volume changes of specimen can be calculated based on volume changes of liquid in the

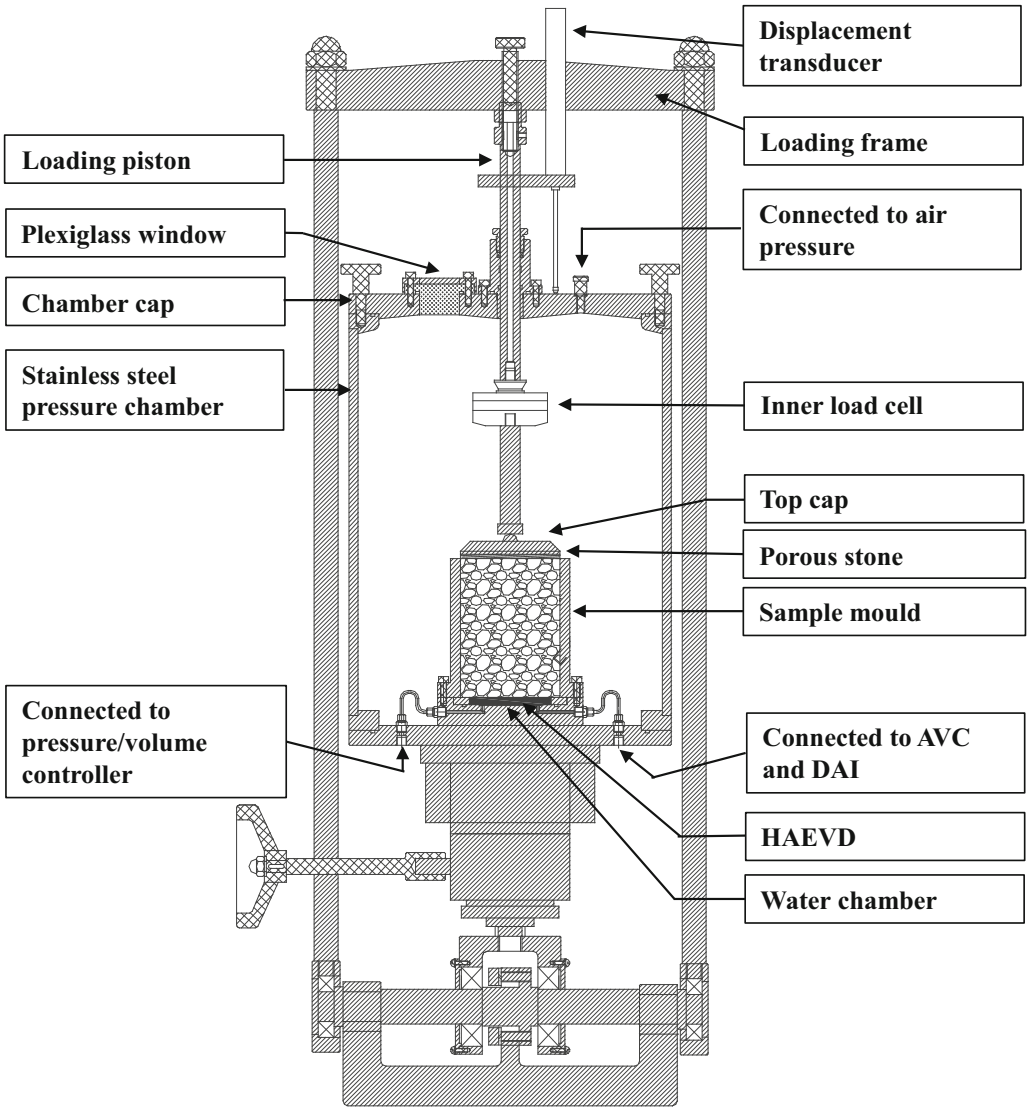

Fig. 3 A schematic layout of the modified oedometer module and oedometer-type modified pressure plate module

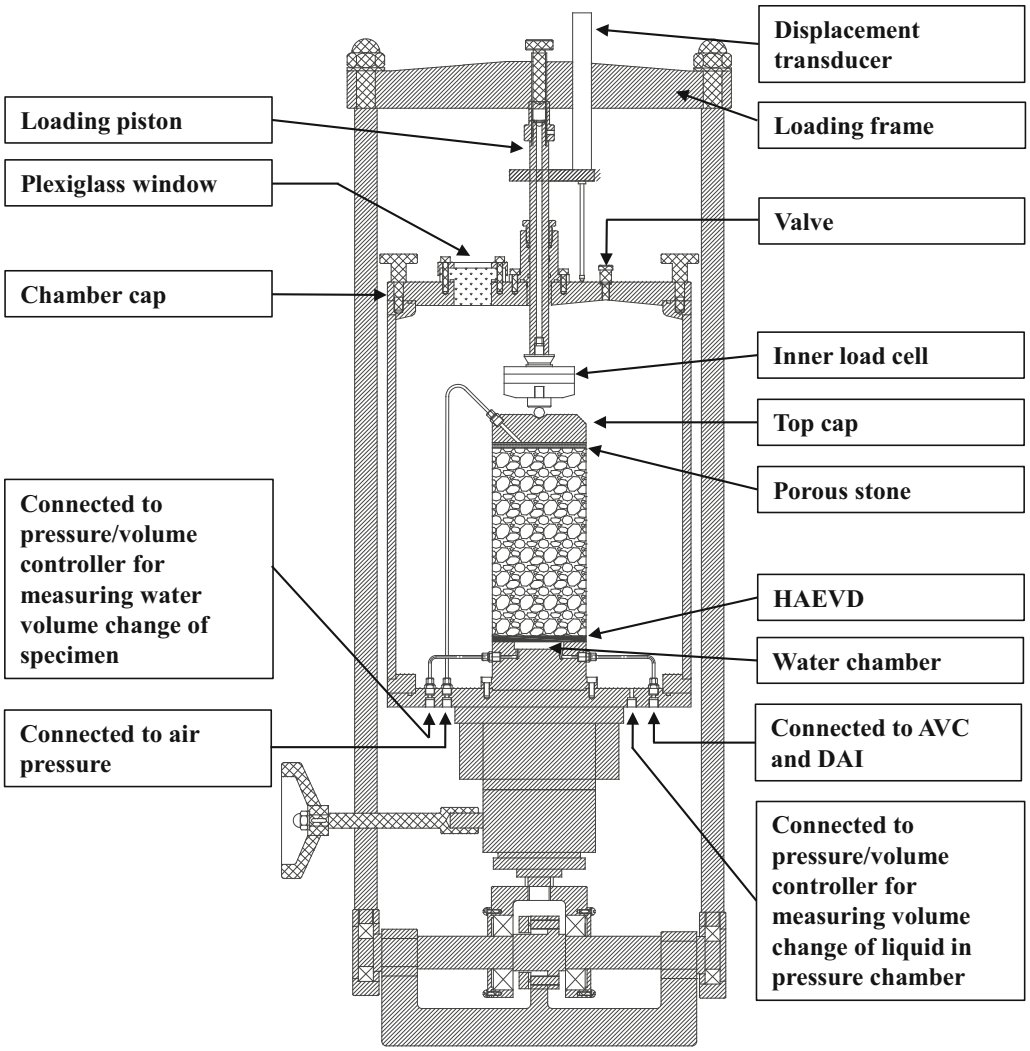

Fig. 4 A schematic layout of the modified triaxial creep module and triaxial-type modified pressure plate module

pressure chamber. A pressure/volume controller connected to the pressure chamber is capable of recording flow-in/-out volume of water while maintaining constant water pressure in the pressure chamber. Thus, the total volume change of the specimen can be indirectly measured by the pressure/volume controller. The two sides of the water chamber are connected to components similar in MPPM. A maximum cell pressure of 2 MPa can be applied in the pressure chamber since the thickness of the pressure chamber is considerable.

2.5 Modified direct shear module

The MDSM was developed based on a soil-soil modified direct shear apparatus described by Hossain and Yin [29]. The fundamental concept of the MDSM is closely related to the previous widely used apparatuses proposed by other researchers [22, 24]. Figure 5 demonstrates the schematic diagram of MDSM. The direct shear box and specimen are installed in the steel pressure chamber. The two sides of the water chamber are connected to components similar in MPPM. The shear load is measured by a load cell in the horizontal direction which is carefully calibrated before the tests. The vertical load is applied by dead weights on the hanger of the lever-arm frame and measured by an inner load cell in the vertical direction. The displacements on horizontal and vertical directions are measured by two calibrated displacement transducers, respectively.

2.6 Modified pressure plate module

Figure 3 presents the schematic layout of the oedometer-type MPPM developed as per apparatuses designed by other researchers [39, 51]. This type of MPPM can be used

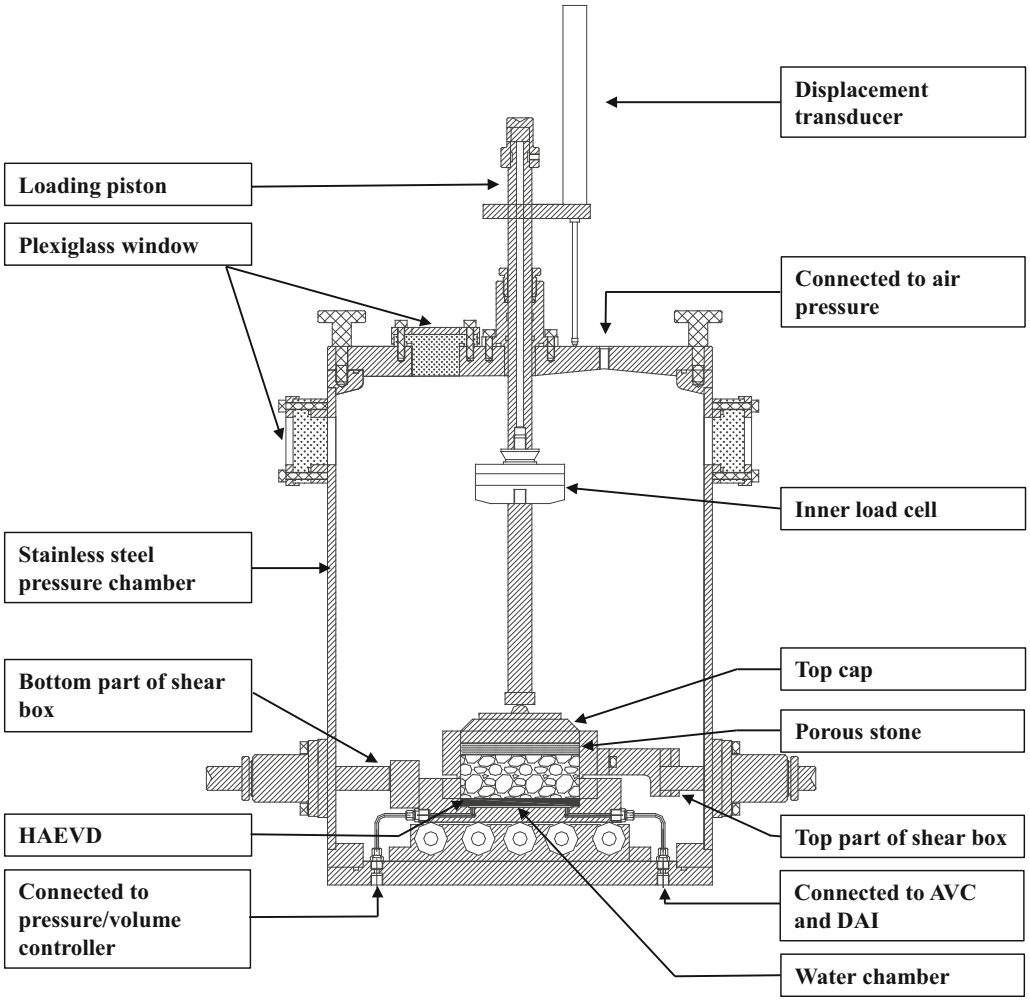

Fig. 5 A schematic layout of the modified direct shear module

to obtain soil WRC with both drying and wetting curves and the drying and wetting scanning curves. Soil WRC affected by net normal stress can be obtained by the oedometer-type MPPM. As shown in Figs. 2a and 3, the samples used in the oedometer-type MPPM are compacted in the sample mould with a thickness of 10 mm. Figure 4 illustrates schematic layout of the triaxial-type MPPM designed following apparatuses proposed by other researchers [48]. Soil WRC affected by net confining pressure can be obtained by the triaxial-type MPPM. The samples used in this module are compacted in a specific mould and placed on the pedestal. Measurement of volume changes of soil during wetting and drying shall be carefully considered based on different soil types. For the expansive clays, lateral shrinkage can occur upon drying under null or low net normal stress in the oedometer-type MPPM. Therefore, the triaxial-type MPPM should be adopted for this specific type of soil, since the volume changes of specimens can be well recorded using the technique of cell liquid measurement described in the introduction section.

2.7 Combinations of different moduli

Figure 6 illustrates a simplified scheme of the pressure-control circuits and most of the pressure transducers. The different module can be easily demounted and installed for different tests. Particularly, the steel pressure chamber is fixed on the support frame and can be used by moduli (MOM and MDSA) in the maintenance of air pressure in unsaturated soil testing. De-aired water is used as the pressurizing medium and filled in the pressure chamber in the MTCM module for the total volume change measurement of specimen in the triaxial creep tests on unsaturated soils. The pressure chamber can be filled with air and de-aired water in oedometer-type MPPM and triaxial-type MPPM, respectively. The pressurized water was applied to the pressure chamber by a bladder air/water cylinder. The

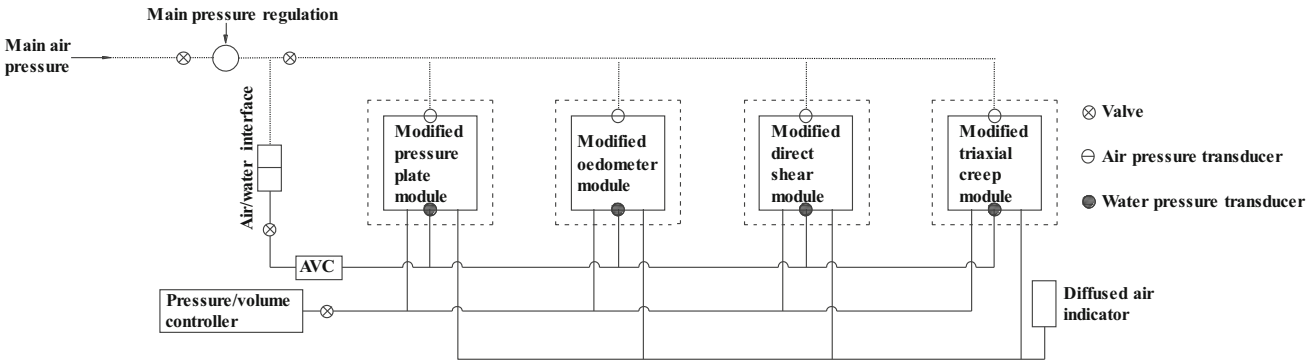

Fig. 6 Scheme of pressure control circuits and transducers of the multifunctional testing apparatus

air and water pressures can be regulated by the pressure panel to deliver certain values of pressure to the system. The same transducers can be used in different moduli, and it is not necessary to demount and install these transducers for different types of tests.

3 Calibration of the multifunctional apparatus

3.1 Calibration of conventional transducers used in the apparatus

Conventional transducers were calibrated following the relevant calibration procedures described in Head [26], including pore-air and pore-water pressure transducers, vertical and horizontal displacement load cells, vertical and horizontal displacement transducers, AVC, and DAI. The temperature during the calibration of apparatus and tests was maintained at 20 °C by several air conditioners in the laboratory. In addition, a dummy sample was used to eliminate the errors of elastic deformation of the frame and bedding effects on the contact surfaces, following the procedures introduced by Head [26] (Fig. 7a).

3.2 Calibration of "immediate" volume change due to pressure increase and "creep" phenomenon

A dummy sample was placed on the pedestal, and the pressure in the pressure chamber was changed for two cycles and maintained for six days to calibrate the chamber expansion (Fig. 7b and c). Figure 7b shows that volume change induced by cell pressure below 100 kPa is relatively larger than those of other pressure values, and this phenomenon has also been observed by other researchers [16, 26, 48]. As shown in Fig. 7c, the volume change can be divided into two components: (i) immediate volume change due to the elastic deformation of the pressure chamber and drainage lines and (ii) volume change with time due to the creep effect of the system. The immediate volume change might be caused by compression of possible trapped air, water compressibility, deformation of membranes or pipelines, and minor pressure chamber distortion. Within common testing period, volume change due to creep effect can be assumed to be linear with time (Fig. 7c). This result agrees well with the previous studies [16, 49]. The volume change due to creep needs to be carefully calibrated and eliminated in the data analysis. The volume change due to the creep effect might result from the minor deformation of the chamber wall, water absorbed by the wall, possible water leakage at some connection parts of this system [16, 26]. The unstable volume change might be caused by the slight temperature changes in the laboratory.

4 Advantages of the multifunctional apparatus

Firstly, a stainless-steel cell has been used as the pressure chamber in the MFA. This steel pressure chamber can be used to measure the total volume changes of specimen in triaxial creep tests on unsaturated soils. Table 3 presents the comparison of calibration results on different testing apparatuses based on cell liquid measurement technique. The comparisons emphasize the ratios of errors to specimen volumes since the volumes of different systems are very different from each other. Compared with some typical double-cell systems [16, 49, 62, 64], the steel pressure chamber has an excellent performance in "creep" volume change under same constant pressure. The calibration coefficient regarding "creep" volume change per week for MFA is about half of the coefficient for a typical double-cell system. This might be due to the simple structure with less water leakage, less water absorption of steel, and

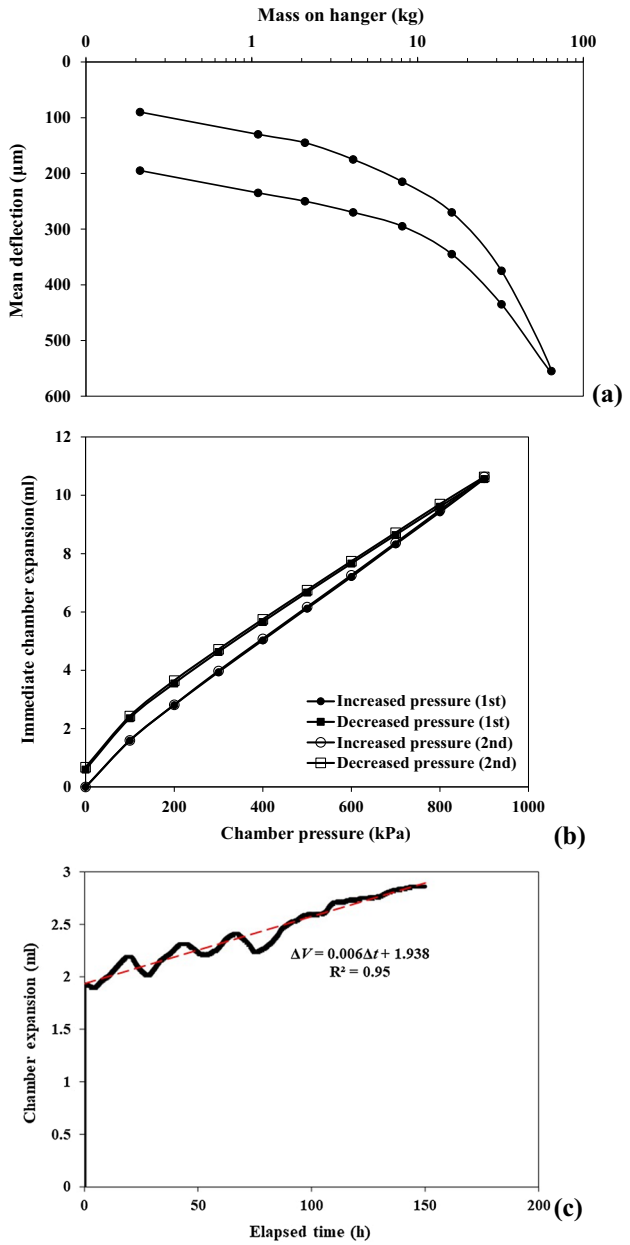

Fig. 7 Calibration curves for **a** elastic deformation of apparatus frame, **b** immediate volume change induced by pressure, and **c** volume change with time

greater stiffness of steel. This minor "creep" volume change is obviously advantageous to the long-period unsaturated soil testing. The performance of "immediate" volume change for the increase of cell pressure is also good, and this error can be easily removed by calibration. Apart from that, the temperature change effect on the steel wall might be less than that on the plexiglass wall. This minor effect might be beneficial in studies of temperature-dependent behaviour of testing materials. Additionally, a maximum cell pressure of 2 MPa can be applied in the pressure chamber because of the competent thickness of the pressure chamber wall. Thus, some triaxial creep tests with high cell pressure could be conducted on this apparatus to study particle breakage behaviour of testing materials. Furthermore, several high-strength and transparent plexiglass windows have been installed on the pressure chamber for real-time observation of the specimen.

Secondly, few studies have focused on the MD of testing apparatus on unsaturated soils. The conventional testing apparatus is very complex and has a lot of different components. Placing four single-function devices for performing different types of tests may take up a lot of space, whereas this MFA may only take up about a quarter of the space of other single-function devices. Furthermore, it is well known that the cost of unsaturated soil testing is high. A very important part of the cost is the expensive test equipment. The expensive test equipment is still a big obstacle for the researchers and engineers to apply the theories in unsaturated soil mechanics to engineering practice. In this MFA, many important parts can be shared in the different test moduli, including pressure chamber, lever-arm frame, support frame, and various transducers. Compared with a single-function device, an MFA can save a lot of money, and several MFAes can be produced at the same cost. It can greatly benefit the popularization of unsaturated soil tests. The utility rate of the MFA is higher than that of a conventional single-function device since it can be used in several different types of tests. Additionally, some calibration results can be shared in the different test moduli, and then, this apparatus can save a lot of time in the calibration. Overall, the apparatus is more feasible for application when compared to the specific single-function devices due to the intrinsic advantages such as space requirements, financial implications, ease of calibration, accuracy, and ease of usage.

Thirdly, although the MFA is currently designed in a manner to enable testing coarse-grained granular materials, the base of the pressure chamber with changeable bottom pedestals on this apparatus can well accommodate specimens with various dimensions. In addition, despite the adoption of ATT in the current design for applying relatively low to medium high suction on granular materials, the apparatus can be potentially modified based on other suction-controlled techniques (e.g. VET) for application of wider suction ranges on clayey soils such as bentonite. Meanwhile, there are reserved channels on the apparatus for future transducers such as fiber bragg grating sensors [63, 64, 66]. Moreover, the pressure chamber is also removable for further improvements of larger chamber to test other large-grained materials.

Table 3 Comparison of calibration results on different testing apparatuses based on cell liquid measurement technique

Type of calibration result	Wheeler [62]	Ng et al. [49]	Yin et al. [68]	Chen et al. [16]	This study
"Immediate" volume change for cell pressure increase from 0 to 500 kPa	700 mm^3 (1.75%)[a]	500 mm^3 (0.5%)[b]	400 mm^3 (0.25%)[c]	4458 mm^3 (0.2%)[d]	6120 mm^3 (0.3%)[d]
"Creep" volume change per week under constant cell pressure of 200 kPa	150 mm^3 (0.125%)[a]	80 mm^3 (0.09%)[b]	–	3141.6 mm^3 (0.2%)[d]	1008 mm^3 (0.06%)[d]

[a]The percentage is assessed based on specimens of diameter 38 mm and height 76 mm

[b]The percentage is assessed based on specimens of diameter 38 mm and height 76 mm

[c]The percentage is assessed based on specimens of diameter 50 mm and height 100 mm

[d]The percentage is assessed based on specimens of diameter 100 mm and height 200 mm

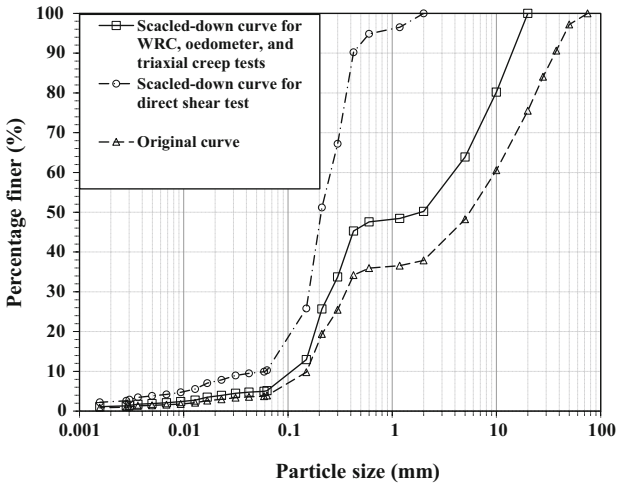

Fig. 8 Particle size distribution curves of the Chongqing granular fill samples used in different types of tests

5 Testing materials, test procedures, results, and discussion

5.1 Testing materials and specimen preparations

The soil utilized in this study was taken from an embankment fill material used for the new Chongqing Airport and categorized as poorly graded gravel with sand [40, 42]. Similar preparation procedures described by Liu et al. [42] were adopted to prepare specimens, including drying, aggregation separation, sieving, drying, water mixing, and compaction. According to the requirements in the Standard BS 1377 [13], the particles larger than 20 mm and 2 mm were removed to obtain a scaled-down curve for the pressure plate, oedometer, and triaxial creep tests and direct shear test (Fig. 8) [42, 55]. Dry density and water content of the prepared specimens were 1.87 Mg/m^3 (88% of maximum dry density) and 5.75%, respectively.

5.2 WRC

Only an oedometer-type pressure plate test was performed in this study. The test was carried out as per ASTM D6836 [4]. The procedures of pressure plate test generally included HAEVD preparation, set-up of specimen, saturation, drying of the specimen, wetting of specimen, demolition of the specimen, and measurement of water content. During the drying part of WRC, the soil suction was increased by steps of increasing the air pressure inside the pressure chamber (Table 4). In each step, the suction was maintained until the drainage of water reached the suction equalization criterion of a rate of 0.02%/day in water content. During the wetting part of WRC, the soil suction was decreased and maintained by steps of decreasing air pressure inside the pressure chamber.

The filter paper method (FPM) can be used as a soil suction sensor to measure the matric and total suction of the soil. This method involves the placement of filter papers against soil specimen from which the pore water flows to the dry filter papers until the hydraulic equilibrium is reached in an airtight container [42]. After the equilibrium, the water content of filter paper is carefully measured, and this water content correlates with the soil suction. The soil suction can be calculated based on the calibration curve of the filter paper. To obtain the WRC of soil, specimens with different targeted water contents are prepared to reach considerable suction range.

WRCs of the granular fill were determined by PPT conducted on this novel MFA and FPM described in Liu et al. [42]. Figure 9 shows comparisons of WRC results obtained by these two methods. The data points obtained from FPM locate approximately in the middle of the drying and wetting paths obtained from PPT. The drying path

Table 4 The suction, net normal stress, and deviatoric stress sequences adopted in different types of tests

Test type	Suction, s (kPa)	Net normal stress, σ_v' (kPa)	Deviatoric stress, q (kPa)
Pressure plate pressure test	0 → 2 → 4 → 6 → 10 → 15 → 20 → 40 → 80 → 100 → 250 → 500 → 250 → 100 → 80 → 40 → 20 → 15 → 10 → 6 → 4 → 2 → 0	0	–
Oedometer test	40	50 → 100 → 200* → 400 → 200 → 100 → 50 → 100 → 200 → 400 → 800* → 1200* → 800 → 400 → 200 → 400 → 800 → 1200	–
Direct shear test	40	100	–
Triaxial creep test	80	150	100 → 200 → 300 → 400

Notes: Arrow denotes loading sequence, and asterisk denotes this loading is maintained for at least one week to investigate the time-dependent compression behaviour

might be a main draining curve, and this path might be a boundary. One FPM data point which is out of the boundary may be caused by the minor error in water content measurement in FPM. Despite imperfect agreement, the WRC results from different methods seem to be comparable. The differences in WRC results might be due to minor errors induced by sample preparations, test processes, and data analysis, such as slight difference in soil density, possible leakage on pipelines, weight of filter paper, and slightly inappropriate calibration curve of filter paper. The so-called "hysteresis" can be observed in the experimental result obtained from PPT. The "hysteresis" means that the drying path is different from the wetting path. The "hysteresis" might be due to several reasons, including differences in the soil–water contact angle between wetting and drying, entrapped air, and connectivity of pores [23]. In the soil pores, large pores can drain first when drying, whereas small pores can be filled first during wetting.

5.3 Unsaturated oedometer test

The main testing procedures described by Chen et al. [17] were adopted in this study, which included HAEVD preparation, set-up of the specimen, saturation, suction equalization, and compression. The rate of 0.02%/day in water content of the specimen was adopted as the equalization criterion in the oedometer test. As listed in Table 4, a series of stepwise increasing vertical loadings were applied on the specimen in a prescribed sequence using a lever-amplified dead weight. The vertical loadings were applied after ensuring the equalization of matric suction on the specimen. All the periods of loadings are at least 48 h and at least one week for the loadings to investigate time-dependent compression behaviour.

Figure 10a to e presents the variations in the void ratio *versus* time (logarithmic scale) for the specimen under matric suction of 40 kPa in the oedometer test. The net vertical stress, σ_v', is defined as follows:

$$\sigma_v' = \sigma_v - u_a \quad (1)$$

where σ_v denotes the total vertical stress and u_a denotes the air pressure.

As shown in Fig. 10a, c and e, the void ratio decreases with the increase of net vertical stress, and the change rate of void ratio increases with the increase of net vertical stress. The soil under different stress levels shows different responses. In general, the changes of void ratio in the secondary compression part are nearly linear with time when net vertical stresses are less than or equal to 400 kPa (Fig. 10a), and those of void ratio in the secondary compression part are nonlinear with time when net vertical stresses are greater than 400 kPa (Fig. 10c). This

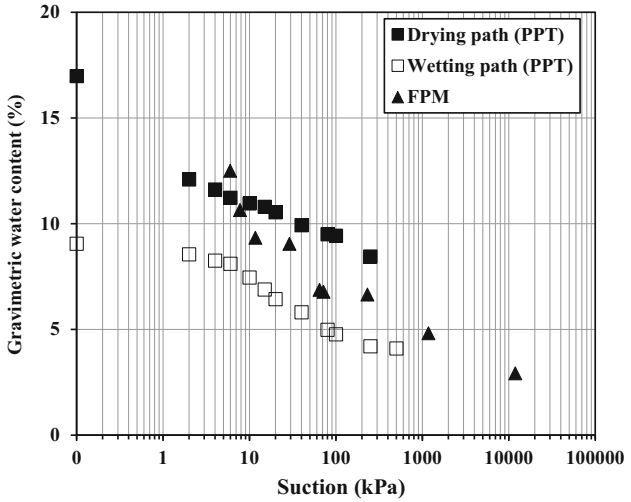

Fig. 9 Comparisons of WRC results obtained by pressure plate test (PPT) and filter paper method (FPM)

difference can be possibly explained by the different compression mechanisms of particles in the specimen. When net vertical stress is not large, the particle contacts between grains can remain stable since the particle friction might be great than the sliding forces at particle contacts. However, particle friction might not be sufficient to maintain the position of the particle if net vertical stress reaches a considerable stress level. At the same time, particle sliding and particle breakage might occur and lead to the rearrangement of soil fabric. Thus, considerable changes in void ratio might occur if net vertical stresses are great. As shown in Fig. 10b and c, the changes in the void ratio are not evident when the net vertical stress is less than the preconsolidation pressure, regardless of unloading or reloading conditions. It is worth noting that this phenomenon can be used to explain a high preconsolidation pressure applied in soil improvement projects can reduce the post-construction settlement of soil layers, especially for granular fills. As shown in Fig. 10b and d, the void ratio increases with the decrease of net vertical stress, and the change rate of the void ratio increases with the increase of net vertical stress. In general, the results agree with those results obtained by Chen et al. [17].

Figure 10f shows the relation of void ratio *versus* net vertical stress in constant-suction oedometer tests. The effective stress, σ'_{vp}, was determined as 316 kPa by the interception point of two fitted lines on the e – log σ'_{vp} curve. This result is consistent with the result described by Chen et al. [17]. Table 5 lists the values of compressibility parameters for the testing materials. The compression index (C_c), and the recompression indices for unloading and reloading loops (C_{r1}, C_{r2}) are defined as follows:

$$C_c, C_{r1} \text{ or } C_{r2} = -\frac{\mathrm{d}(e)}{d(\log(\sigma'_v))} \tag{2}$$

where e denotes the void ratio and σ'_v denotes the net vertical stress.

The creep coefficient, $C_{\alpha e}$, is defined by the equation as follows:

$$C_{\alpha e} = -\frac{\mathrm{d}(e)}{\log(t/t_0)} \quad (t > t_0) \tag{3}$$

where t_0 denotes the time corresponding to the end of the transient period and is taken as 2 min in this study and d(e) denotes change of void ratio from the time t_0. As listed in Table 5, the C_c, C_{r1}, and C_{r1} values are 0.07, 0.002, and 0.004, respectively. The $C_{\alpha e}$ values for net vertical stresses of 200 kPa, 800 kPa, and 1200 kPa are 0.0003, 0.0011, and 0.0011, respectively. The slight differences between the compressibility parameters and those obtained by Chen et al. [17] might be caused by the inherent anisotropy induced by specimen preparation and the complex behaviour of coarse-grained granular materials [41]. In general, compared with the behaviour of fine-grained granular material, the behaviour of coarse-grained granular materials is very complex and highly heterogeneous, and this behaviour might easily cause non-uniform experimental results [54, 56, 58, 65, 67].

5.4 Unsaturated direct shear test

The testing procedures suggested by Borana et al. [9–11] were adopted in this study, which included HAEVD preparation, set-up of specimen, saturation, suction equalization, and drained shearing at constant suction and net normal stress. The calculated axial load, air pressure in the pressure chamber, and water pressure under HAEVD were applied sequentially in the suction equilibration stage (Table 4). Constant vertical deformation and water flow rate of 0.02%/day in water content of specimen were adopted as the equalization criteria. In the shearing stage, the specimen was sheared at a constant rate of 0.004 mm/min until the horizontal displacement reached 12 mm.

Figure 11 shows the result of the direct shear test on specimens under suction of 40 kPa and net normal stress of 100 kPa. Based on the relation between shear stress and horizontal displacement, soil shows gradually hardening behaviour. In the curve of vertical displacement and horizontal displacement, soil shows compression when the horizontal displacement is approximately less than 3%, followed by a little dilation. This dilation behaviour might be attributed to the application of suction on the specimen. Similar phenomena have been observed by Hossain and Yin [28] in a compacted completely decomposed granite soil. In general, the results agree with the results reported

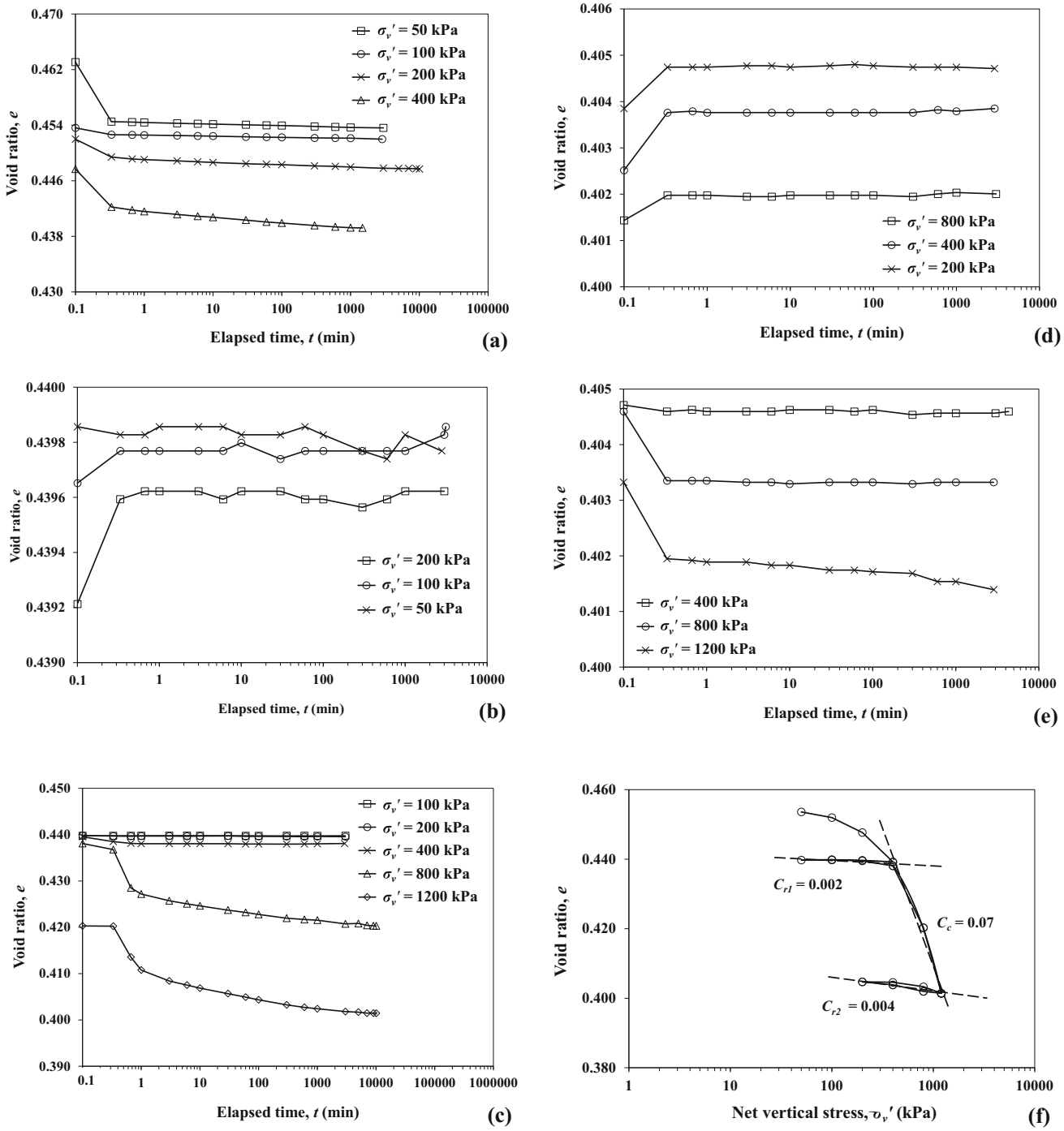

Fig. 10 Results of oedometer test on Chongqing granular fill under suction of 40 kPa: **a** σ_v' is loaded from 50 to 400 kPa, **b** σ_v' is unloaded from 400 to 50 kPa, **c** σ_v' is reloaded from 50 to 400 kPa and loaded from 400 to 1200 kPa, **d** σ_v' is unloaded from 1200 to 200 kPa, **e** σ_v' is reloaded from 200 to 1200 kPa, and **f** void ratio *versus* net vertical stress

by Borana [9–11]. Under a certain level of net normal stress, the higher the suction, the more the shear dilation. Additionally, the softening and hardening behaviour of the soil is not evident with the changes of suction.

5.5 Unsaturated triaxial creep test

The procedures introduced by Lai et al. [34] were adopted, which included HAEVD preparation, set-up of the

Table 5 Values of compressibility parameters for the testing materials based on oedometer test

Parameter	Unit	Value
Compression index (C_c)	–	0.07
Recompression index (C_{r1})	–	0.002
Recompression index (C_{r2})	–	0.004
Creep coefficient ($C_{\alpha e}$) for σ_v' = 200 kPa	–	0.0003
Creep coefficient ($C_{\alpha e}$) for σ_v' = 800 kPa	–	0.0011
Creep coefficient ($C_{\alpha e}$) for σ_v'= 1200 kPa	–	0.0011

specimen, equalization, isotropic consolidation, and loading under a certain matric suction. The termination criterion of the suction equilibration stage was the flow rate of 0.02%/day in water content. After the equalization stage, the isotropic consolidation was applied by increasing the confining pressure to obtain a desired net confining stress (150 kPa). The multi-stage loading method was adopted in this study, which was used by many researchers for the investigation of the creep behaviour of soils [34]. The deviatoric stresses for all the stages are listed in Table 4. When the axial deformation rate reached 0.005 mm/day, the stabilization of relevant axial deformation at certain deviatoric stress was obtained. The shear strength of specimens was determined as 500 kPa before the triaxial creep tests by the reanalysis of results from Liu et al. [42]. The deviatoric stress level, $D=\frac{(\sigma_1-\sigma_3)}{(\sigma_1-\sigma_3)_f}$, is defined as the ratio of applied deviatoric stress, $(\sigma_1-\sigma_3)$, to maximum deviatoric stress, $(\sigma_1-\sigma_3)_f$.

Figure 12a and b presents the curves of axial strain *versus* time and axial strain rate *versus* time for the specimen (s = 80 kPa; σ_v' = 150 kPa) measured at different deviatoric stress levels. The axial strain rate, $\dot{\varepsilon}_a$, is defined by the equation as follows:

$$\dot{\varepsilon}_a = \frac{d\varepsilon_a}{dt} \tag{4}$$

where $d\varepsilon_a$ is the variation of axial strain measured over the corresponding period dt.

Figure 12a shows that, after 10 min, the axial strain increases linearly with time when the D is less than or equal to 0.6. However, the axial strain increases nonlinearly with time after 10 min when the D is at 0.8. A similar phenomenon can be observed in the oedometer tests. This might be due to the different compression mechanisms of particles explained in the section of explanation of oedometer test results. Figure 12b presents the variation of axial strain rate with time. It seems that the axial strain rate decreases linearly with time except for a few date points. The equation suggested by Singh and Mitchell [57] was

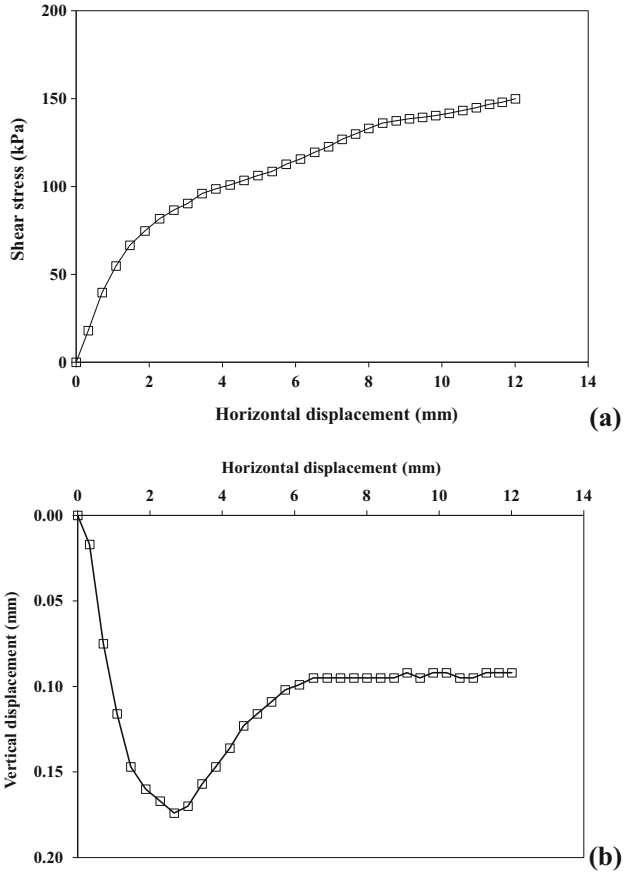

Fig. 11 Results of direct shear test on Chongqing granular fill under suction of 40 kPa and net normal stress of 100 kPa: **a** shear stress *versus* horizontal displacement curve and **b** vertical displacement *versus* horizontal displacement curve

used to calculate the linear trend of axial strain rate with time as follows:

$$m = -\frac{\Delta \log(\dot{\varepsilon}_a)}{\Delta \log(t)} \tag{5}$$

where m denotes the slope of the linear trend line, $\dot{\varepsilon}_a$ denotes axial strain rate, and t denotes period.

Based on the fitting results, the m-value for deviatoric stress levels ranging from 0.2 to 0.8 is 0.98, 1.02, 1.05, and 1.15, respectively. Singh and Mitchell [57] suggested that the slope was constant regardless of the variable deviatoric stress level and time for a given soil. However, Lai et al. [34] found the convergence of straight lines of the axial strain rate with elapsed time in an unsaturated clay. As shown in Fig. 12b, a similar convergent trend can be observed in different deviatoric stress levels, and this trend means that the slope increases with the increase of deviator stress level and is not constant with elapsed time. It agrees with the observations suggested by other researchers [34].

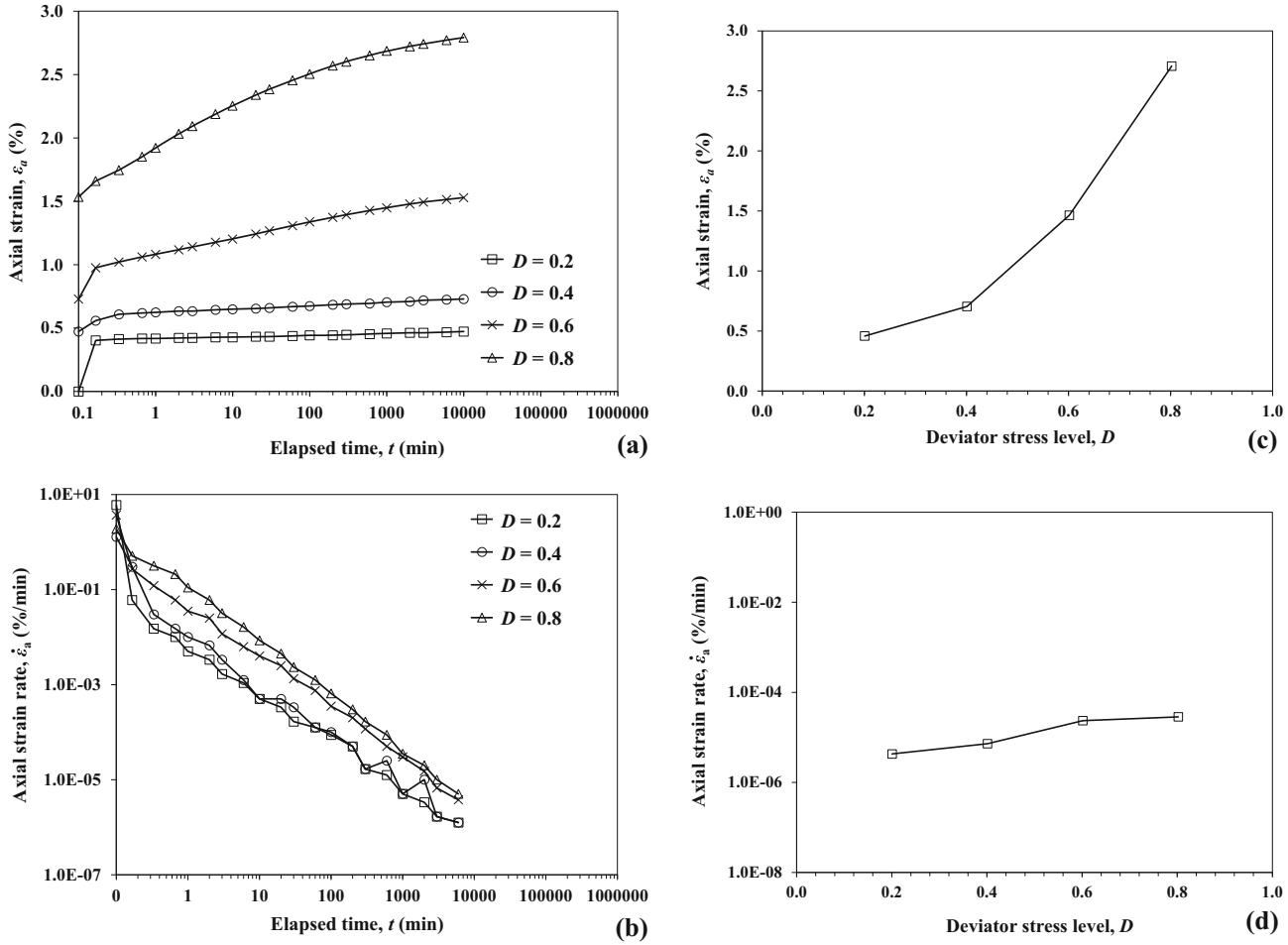

Fig. 12 Results of triaxial creep test on Chongqing granular fill under suction of 80 kPa and net confining pressure of 150 kPa: **a** axial strain *versus* time curve, **b** axial strain rate *versus* time curve, **c** axial strain *versus* stress level relationship, and **d** axial strain rate *versus* stress level relationship

Figure 12c and d shows relationship between axial strain or axial strain rate and deviatoric stress level at period of 24 h. The axial strain increases with the increasing deviator stress level. Additionally, it appears that the axial strain rate increases linearly with the increase of deviator stress level. A similar trend was found by Mesri et al. [45] in saturated clay and Lai et al. [34] in unsaturated clay. In general, it is noted that the MFA works very well in establishing the creep parameters for unsaturated soils precisely.

6 Conclusion

A novel state-of-the-art modular-design-based MFA is designed and manufactured for performing a variety of tests such as pressure plate test, oedometer test, direct shear test, and triaxial creep test on unsaturated soils. The individual module, typical calibration results, and advantages are presented and discussed. A series of tests under different stress state variables have been conducted, and the testing process and methodologies are furnished. The calibration coefficient regarding "creep" volume change per week for MFA is about half of the coefficient for a typical double-cell system. Besides, the apparatus is more feasible for application when compared to the specific single-function devices due to the intrinsic advantages such as space requirements, financial implications, ease of calibration, accuracy, and ease of usage. Furthermore, the MFA is designed in a manner to enable testing specimens with different dimensions and to control soil suction based on different techniques. Overall, it is observed that MFA is suitable to perform any of the tests for unsaturated soils, as listed above.

The soil type and stress path of validation tests are relatively simple. In addition, other types of suction-controlled techniques can be adopted in the future modifications to apply and maintain a wider suction range on different types of soils. Moreover, the temperature effect on volume change shall be carefully considered if the apparatus is used in an environment without constant temperature control. Finally, there is a limitation in the determination of volume change of specimen under null or low net normal stress in the oedometer-type MPPM. Future studies shall be conducted to avoid this limitation in testing some special types of soils, especially for expansive clays which have lateral shrinkage during drying.

Acknowledgements The work in this paper was supported by General Research Fund (GRF) (PolyU 152209/17E, PolyU 152179/18E, PolyU 152130/19E) and a Research Impact Fund (R5037-18) from Research Grants Council of Hong Kong Special Administrative Region Government of China. The work was also supported by grants (ZVNC and ZDBS) from the Hong Kong Polytechnic University, China. We also acknowledge the supports by Research Institute for Sustainable Urban Development of the Hong Kong Polytechnic University (PolyU) and Center for Urban Geohazard and Mitigation of Faculty of Construction and Environment of PolyU. The helpful discussions with Mr. Jia-Feng Mao from the Nanjing Soil Instrument Factory Co., Ltd., are also gratefully acknowledged.

References

1. Adams BA, Wulfsohn D, Fredlund DG (1996) Air volume change measurement in unsaturated soil testing using a digital pressure-volume controller. Geotech Test J 19(1):12–21
2. Agus SS, Leong EC, Rahardjo H (2000) A triaxial permeameter for unsaturated soils. In Unsaturated soils for Asia. Proceedings of the Asian Conference on Unsaturated Soils, UNSAT-ASIA 2000, Singapore, 18–19 May 2000 (pp. 365–370). AA Balkema
3. Agus SS, Schanz T (2005) Comparison of four methods for measuring total suction. Vadose Zone J 4(4):1087–1095
4. ASTM D 6836 (2016) Standard test methods for determination of the soil water characteristic curve for desorption using hanging column, pressure extractor, chilled mirror hygrometer, or centrifuge. ASTM International, West Conshohocken
5. Aversa S, Nicotera MV (2002) A triaxial and oedometer apparatus for testing unsaturated soils. Geotech Test J 25(1):3–15
6. Baldwin CY, Clark KB (2000) Design rules: the power of modularity (Vol 1). MIT Press, Cambridge
7. Bernier F, Volckaert G, Alonso E, Villar M (1997) Suction-controlled experiments on Boom clay. Eng Geol 47(4):325–338
8. Bishop AW and Donald IB (1961) The experimental study of partly saturated soil in the triaxial apparatus. In Proc. 5th Int. Conf. Soil Mech. Found. Eng., Paris, Vol. 1, pp. 13–21
9. Borana L, Yin JH, Singh DN, Shukla SK (2015) A modified suction-controlled direct shear device for testing unsaturated soil and steel plate interface. Mar Georesources Geotechnol 33(4):289–298
10. Borana L, Yin JH, Singh DN, Shukla SK (2016) Interface behavior from suction-controlled direct shear test on completely decomposed granitic soil and steel surfaces. Int J Geomech 16(6):D4016008
11. Borana L, Yin JH, Singh DN, Shukla SK, Tong F (2018) Direct shear testing study of the interface behavior between steel plate and compacted completely decomposed granite under different vertical stresses and suctions. J Eng Mech 144(1):04017148
12. Boso M, Tarantino A, Mongiovi L (2005) A direct shear box improved with the osmotic technique, Proceedings of advanced experimental unsaturated soil mechanics, Trento, pp. 85–91
13. British Standards Institution (BSI) (1990) Methods of test for soils for civil engineering purposes. BS 1377, BSI, London
14. Bulut R, Leong EC (2008) Indirect measurement of suction. Geotech Geol Eng 26(6):633–644
15. Chen R (2007) Experimental study and constitutive modelling of stress-dependent coupled hydraulic hysteresis and mechanical behaviour of an unsaturated soil. PhD thesis, Hong Kong University of Science and Technology, Hong Kong, China
16. Chen WB, Yin JH, Feng WQ (2019) A new double-cell system for measuring volume change of a soil specimen under monotonic or cyclic loading. Acta Geotech 14(1):71–81
17. Chen WB, Liu K, Feng WQ, Borana L, Yin JH (2020) Influence of matric suction on nonlinear time-dependent compression behavior of a granular fill material. Acta Geotech 15(3):615–633
18. Clayton CR, Khatrush SA, Bica AVD, Siddique A (1989) The use of Hall effect semiconductors in geotechnical instrumentation. Geotech Test J 12(1):69–76
19. Delage P, Howat MD, Cui YJ (1998) The relationship between suction and swelling properties in a heavily compacted unsaturated clay. Eng Geol 50(1–2):31–48
20. Delage P, Romero E, Tarantino A (2008) Recent developments in the techniques of controlling and measuring suction in unsaturated soils. In Keynote Lecture, Proc. 1st Eur. Conf. on Unsaturated Soils (pp. 33–52)
21. Delage P, Suraj De Silva GPR, Vicol T (1992) Suction controlled testing of non-saturated soils with an osmotic consolidometer. In: 7th International conference on expansive soils, pp. 206–211
22. Escario V (1980) Suction controlled penetration and shear tests. In Expansive Soils (pp. 781–797). ASCE
23. Fredlund DG, Rahardjo H (1993) Soil mechanics for unsaturated soils. Wiley, New York
24. Gan JKM, Fredlund DG, Rahardjo H (1988) Determination of the shear strength parameters of an unsaturated soil using the direct shear test. Can Geotech J 25(3):500–510
25. Hamidi A, Habibagahi G, Ajdari M (2013) A modified osmotic direct shear apparatus for testing unsaturated soils. Geotech Test J 36(1):20–29
26. Head KH (1998) Manual of soil laboratory testing. Wiley, New York
27. Hilf JW (1956) An investigation of pore-water pressure in compacted cohesive soils. PhD thesis, Technical Memorandum. No. 654, U.S. Department of the Interior, Bureau of Reclamation, Design and Construction Division, Denver, CO, US
28. Hossain MA, Yin JH (2010) Behavior of a compacted completely decomposed granite soil from suction controlled direct shear tests. J Geotech Geoenviron Engng 136(1):189–198
29. Hossain MA, Yin JH (2014) Behaviour of a pressure-grouted soil-cement interface in direct shear tests. Int J Geomech 14(1):101–109
30. Houston SL, Houston WN, Wagner AM (1994) Laboratory filter paper suction measurements. Geotech Test J 17(2):185–194
31. Jose A, Tollenaere M (2005) Modular and platform methods for product family design: literature analysis. J Intell Manuf 16(3):371–390
32. Klotz EU, Coop MR (2002) On the identification of critical state lines for sands. Geotech Test J 25(3):289–302
33. Krahn J, Fredlund DG (1972) On total, matric and osmotic suction. J Soil Sci 114(5):339–348
34. Lai XL, Wang SM, Ye WM, Cui YJ (2014) Experimental investigation on the creep behavior of an unsaturated clay. Can Geotech J 51(6):621–628

35. Laudahn A, Sosna K, Boháč J (2005) A simple method for air volume change measurement in triaxial tests. Geotech Test J 28(3):313–318
36. Lauer C, Engel J (2005) A triaxial device for unsaturated sand-New Developments. In: Unsaturated Soils: Experimental Studies (pp. 301–314). Springer, Berlin, Heidelberg
37. Li J, Yin ZY, Cui YJ, Hicher PY (2017) Work input analysis for soils with double porosity and application to the hydromechanical modeling of unsaturated expansive clays. Can Geotech J 54(2):173–187
38. Li J, Yin ZY, Cui YJ, Liu K, Yin JH (2019) An elasto-plastic model of unsaturated soil with an explicit degree of saturation-dependent CSL. Eng Geol 260:105240
39. Lins Y, Schanz T, Fredlund DG (2009) Modified pressure plate apparatus and column testing device for measuring SWCC of sand. Geotech Test J 32(5):450–464
40. Liu K, Chen WB, Feng WQ, Yin JH (2017) Experimental study on the unsaturated behaviour of a compacted soil. In: 7th International Conference on Unsaturated Soils (UNSAT2018), 3rd - 5th August 2018, The Hong Kong University of Science and Technology (HKUST)
41. Liu K, Yin ZY, Chen WB, Feng WQ, Yin JH (2021) Nonlinear model for the stress–strain–strength behavior of unsaturated granular materials. Int J Geomech 21(7):04021103
42. Liu K, Yin JH, Chen WB, Feng WQ, Zhou C (2020) The stress-strain behaviour and critical state parameters of an unsaturated granular fill material under different suctions. Acta Geotech 15:3383–3398
43. Madsen HB, Jensen CR, Boysen T (1986) A comparison of the thermocouple psychrometer and the pressure plate methods for determination of soil water characteristic curves. J Soil Sci 37:357–362
44. Marinho FAM, Take WA, Tarantino A (2008) Measurement of matric suction using tensiometric and axis translation techniques. Geotech Geol Eng 26(6):615–631
45. Mesri GRES, Febres-Cordero E, Shields D, Castro A (1981) Shear stress-strain-time behaviour of clays. Géotechnique 31(4):537–552
46. Monroy R, Zdravkovic L, Ridley AM (2015) Mechanical behaviour of unsaturated expansive clay under K0 conditions. Eng Geol 197(30):112–131
47. Nishimura T (2016) Investigation on creep behavior of geo-materials with suction control technique. In: E3S Web of Conferences (Vol. 9, p. 18002). EDP Sciences
48. Ng CWW, Lai CH, Chiu CF (2012) A modified triaxial apparatus for measuring the stress path-dependent water retention curve. Geotech Test J 35(3):490–495
49. Ng CW, Zhan LT, Cui YJ (2002) A new simple system for measuring volume changes in unsaturated soils. Can Geotech J 39(3):757–764
50. Nichol C, Smith L, Beckie R (2003) Long-term measurement of matric suction using thermal conductivity sensors. Can Geotech J 40(3):587–597
51. Perez-Garcia N, Houston SL, Houston WN, Padilla JM (2008) An oedometer-type pressure plate SWCC apparatus. Geotech Test J 31(2):115–123
52. Rahardjo H, Fredlund D (1996) Consolidation apparatus for testing unsaturated soils. Geotech Test J 19(4):341–353
53. Sheng DC (2011) Review of fundamental principles in modelling unsaturated soil behaviour. Comput Geotech 38(6):757–776
54. Shi XS, Gao YF, Ding JW (2021) Estimation of the compression behavior of sandy clay considering sand fraction effect based on equivalent void ratio concept. Eng Geol 280:105930
55. Shi XS, Liu K, Yin JH (2021) Effect of initial density, particle shape, and confining stress on the critical state behavior of weathered gap-graded granular soils. J Geotech Geoenviron Engng 147(2):04020160
56. Shi XS, Zhao JD, Gao Y (2021) A homogenization-based state-dependent model for gap-graded granular materials with fine-dominated structure. Int J Numer Anal Methods Geomech 45(8):1007–1028
57. Singh A, Mitchell JK (1968) General stress-strain-time function for soils. J Soil Mech Found Div 94(1):21–46
58. Tang JY, Xu DS, Liu HB (2018) Effect of gravel content on shear behavior of sand-gravel mixture. Rock Soil Mech 39(1):93–102 (**in Chinese**)
59. Tarantino A, Gallipoli D, Augarde CE et al (2011) Benchmark of experimental techniques for measuring and controlling suction. Géotechnique 61(4):303–312
60. Ulrich K (1995) The role of product architecture in the manufacturing firm. Res Policy 24(3):419–440
61. Villar MV (1999) Investigation of the behaviour of bentonite by means of suction-controlled oedometer tests. Eng Geol 54(1–2):67–73
62. Wheeler SJ (1988) The undrained shear strength of soils containing large gas bubbles. Géotechnique 38(3):399–413
63. Xu DS (2017) A new measurement approach for small deformations of soil specimens using fiber bragg grating sensors. Sensors 17(5):1016
64. Xu DS, Borana L, Yin JH (2014) Measurement of small strain behavior of a local soil by fiber Bragg grating-based local displacement transducers. Acta Geotech 9(6):935–943
65. Xu DS, Huang M, Zhou Y (2020) One-dimensional compression behavior of calcareous sand and marine clay mixtures. Int J Geomech 20(9):04020137
66. Xu DS, Liu HB, Luo WL (2018) Development of a novel settlement monitoring system using fiber-optic liquid-level transducers with automatic temperature compensation. IEEE Trans Instrum Meas 67(9):2214–2222
67. Xu DS, Liu HB, Rui R, Gao Y (2019) Cyclic and postcyclic simple shear behavior of binary sand-gravel mixtures with various gravel contents. Soil Dyn Earthq Eng 123:230–241
68. Yin JH (2003) A double cell triaxial system for continuous measurement of volume changes of an unsaturated or saturated soil specimen in triaxial testing. Geotech Test J 26(3):353–358